



An update on coating/manufacturing techniques of microneedles

Tamara N. Tarbox¹ · Alan B. Watts¹ · Zhengrong Cui¹ · Robert O. Williams III¹

Published online: 29 December 2017
© Controlled Release Society 2017

Abstract

Recently, results have been published for the first successful phase I human clinical trial investigating the use of dissolving polymeric microneedles... Even so, further clinical development represents an important hurdle that remains in the translation of microneedle technology to approved products. Specifically, the potential for accumulation of polymer within the skin upon repeated application of dissolving and coated microneedles, combined with a lack of safety data in humans, predicates a need for further clinical investigation. Polymers are an important consideration for microneedle technology—from both manufacturing and drug delivery perspectives. The use of polymers enables a tunable delivery strategy, but the scalability of conventional manufacturing techniques could arguably benefit from further optimization. Micromolding has been suggested in the literature as a commercially viable means to mass production of both dissolving and swellable microneedles. However, the reliance on master molds, which are commonly manufactured using resource intensive microelectronics industry-derived processes, imparts notable material and design limitations. Further, the inherently multi-step filling and handling processes associated with micromolding are typically batch processes, which can be challenging to scale up. Similarly, conventional microneedle coating processes often follow step-wise batch processing. Recent developments in microneedle coating and manufacturing techniques are highlighted, including micromilling, atomized spraying, inkjet printing, drawing lithography, droplet-born air blowing, electro-drawing, continuous liquid interface production, 3D printing, and polyelectrolyte multilayer coating. This review provides an analysis of papers reporting on potentially scalable production techniques for the coating and manufacturing of microneedles.

Keywords Microneedles · High throughput · Dissolving microneedles · Inkjet printing · Micromolding

Introduction

The skin is an effective barrier that protects the body from external elements including microbes, foreign chemicals, injury, and dehydration [1]. For an adult, the surface area of the skin comprises approximately 2 m² or about 15% of the body mass [2], providing a sizable area for the potential delivery or administration of therapeutics. There are a number of reasons to deliver therapeutic agents by way of the skin. For patients who have difficulty swallowing pills or are unconscious or otherwise incapacitated, topical/transdermal application of medicine is a welcomed alternative to the oral route. Also, the simple and painless nature of certain dermal and transdermal drug applications leads

to improved patient acceptance and compliance, thereby reducing overall costs associated with treatment [3]. However, the lipophilic character and physical structure of the stratum corneum (SC) selectively limit skin permeability, the exact nature of which is described elsewhere [2, 4].

In 1998, Henry et al. first reported the use of microneedles (MNs) as a “painless” means to increase the permeability of excised human skin to calcein, a model drug, by up to four orders of magnitude [5]. These silicon microprojections were designed to be long enough to breach the SC but short enough to avoid deeper regions of the skin where pain receptors reside. For this study, they used reactive ion etching (RIE) to fabricate an array of sharp 150 μm-long MNs. By definition, MNs are needle-like structures with a maximum length of 1 mm [6]. MNs longer than 1 mm have been investigated, and while they were associated with increased pain during application, that level of pain was still less than that compared to a conventional 26-gauge hypodermic needle [7]. Less pain generally translates to improved patient acceptance and compliance, as supported in a study by Arya et al., in which the majority of subjects preferred

✉ Tamara N. Tarbox
tamara.tarbox@austin.utexas.edu

¹ College of Pharmacy, University of Texas at Austin, Austin, TX, USA

the use of a MN patch over intramuscular injection, which was rated as more painful [8].

With the results from the first successful phase I clinical trial for a therapeutic application of dissolving MNs published [9], dissolving MN products in development are poised for rapid expansion. Dissolving MNs [10–15] and MN coatings [16–18] have been manufactured from various biocompatible materials that dissolve or biodegrade, such as natural and synthetic polymers and sugars. A number of manufacturing techniques have been applied to MN production, with the original techniques emerging from the microelectronics industry due to the early development of precision and submicron resolution capabilities [19]. While the RIE method reported by Henry et al. did successfully result in ordered microneedle arrays capable of penetrating the SC for increased drug permeability, the manufacturing process included eight different steps involving specialized equipment and/or materials to prepare the silicon wafer for the actual etching step [5]. The material and design limitations of microelectromechanical systems (MEMS) techniques like RIE, combined with costly equipment and processing condition requirements [20, 21], have led to a need for more readily adaptable and cost-effective manufacturing techniques for MN production.

Numerous reviews describing different aspects of MN technology have been published on such topics as materials [22], delivery strategies [23–25], fabrication [19, 26], designs [10, 27], feasibility [28], characterization [29], safety [30], and clinical trials [31]. However, no review could be found that focuses on the practical use of more recently developed or adapted technologies featuring polymers in the manufacturing/coating of MNs such as micromilling [20, 32], atomized spraying or inkjet printing into molds [14, 33], droplet-born air blowing [34], electro-drawing [35], drawing lithography [36], 3D printing [37], continuous liquid interface production [38], inkjet printing [39–41], and polyelectrolyte multilayer coating [42–44]. Therefore, this review is intended to provide a tool to guide the development of MNs using biocompatible dissolving or biodegradable materials in drug delivery systems, with a focus on more recent improvements in manufacturing technology and associated regulatory aspects, to enable rapid and cost-effective scale-up.

The state of microneedles

Types of microneedles

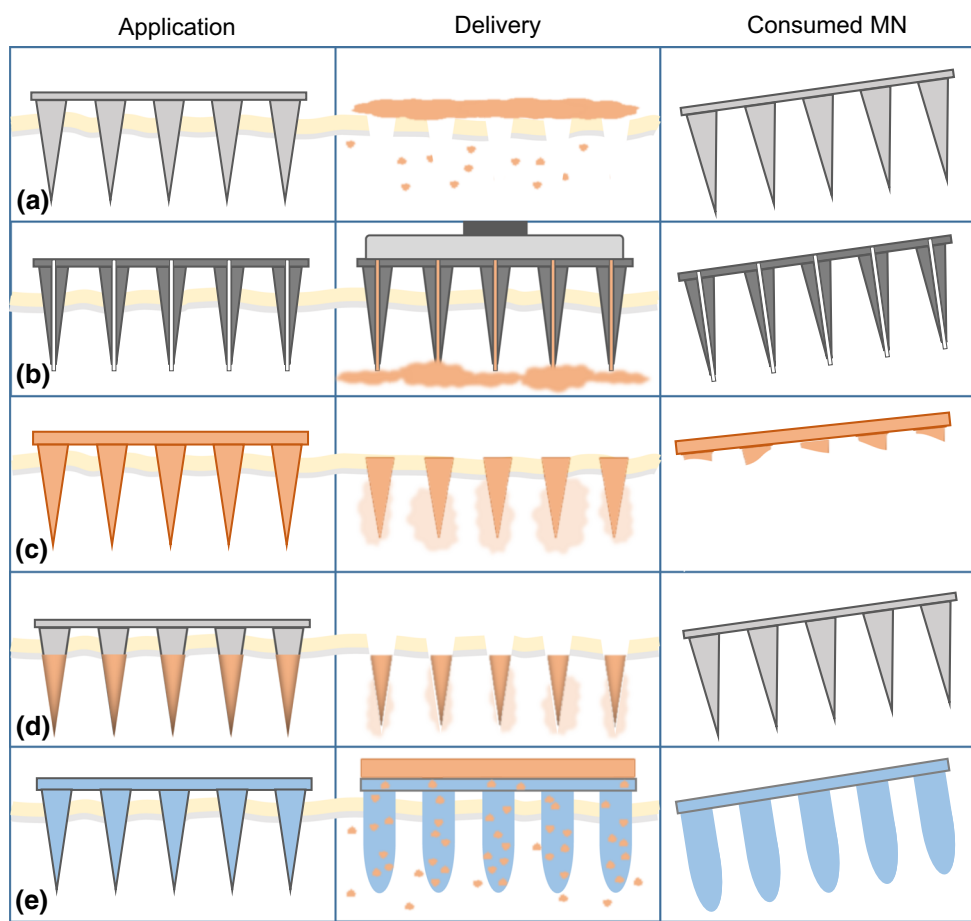
Briefly, MNs are generally grouped into five types: solid, hollow, dissolving, coated, and swellable, and the uses of them are illustrated in Fig. 1. Solid MNs (Fig. 1(a)) apply the best advantage of MNs, which is to painlessly penetrate the SC. As shown in Fig. 1a, the use of solid MNs is followed by the application of a therapeutic agent (i.e., in a gel, cream, or

patch) that can then permeate the skin through the transient MN-generated pores [45]. Hollow MNs (Fig. 1(b)) are much like miniaturized versions of hypodermic needles, through which drug solution can be delivered transdermally. Notable differences between hollow microneedles and hypodermic needles include reduced pain with MNs [46], more pressure required to achieve flow through the MNs [46], and the risk for clogging of the MN microchannels [47]. Unlike solid or hollow MNs, dissolving MNs (Fig. 1(c)) are intended to be left in the skin to release the therapeutic agent, so there is little to no waste remaining after use. Dissolving MNs have been designed for rapid bolus delivery [48] or for extended release over time [49]. Coated MNs (Fig. 1(d)) are designed to penetrate the SC to carry and deposit a therapeutic agent within the skin, sometimes within seconds, after which the MNs are removed [16, 44, 50]. Coatings have also been designed to persist in the skin for sustained release of the active ingredient [44, 51]. Swellable MNs (Fig. 1(e)) are fabricated from crosslinked hydrogels and swell with interstitial fluid but do not dissolve in the skin and are therefore removed after application. These MNs have been combined with a patch to release drug in the skin [52, 53] as shown in Fig. 1e or to collect fluid for sampling [54]. The summary of MN application, delivery of therapeutics, and consumed MN by type in Fig. 1 highlights the similarities of the five MN types to pierce the SC for transdermal drug administration and differences in the remaining MN product after use. Solid, hollow, and coated MNs are intact after use, whereas dissolving MNs are essentially consumed, and swellable MNs are no longer sharp after use.

Advantages and limitations of dissolving, coated, and swellable microneedles

Polymers have been used in the manufacture of all five types of MNs, with the development of dissolving, coated, and swellable MN applications relying heavily on the use of biocompatible dissolving and biodegradable materials. The advantages and limitations of these three types of MNs are summarized in Table 1. One major advantage for dissolving MNs, as seen in Fig. 2, is flexibility in drug loading. This type of MN has the capacity for loading a large amount of drug. Drugs can be loaded throughout the array (Fig. 2(a)) [55], limited to layers (Fig. 2(b, c)) [14] or to microparticles within the needles (Fig. 2(d)) [49], or isolated within the tips (Fig. 2(e)) [49, 56, 57]. Because these MNs dissolve in the skin, there is a lack of potentially dangerous sharps waste [14]. However, the safety of long-term repeated intradermal exposure to these materials in humans has not been established and therefore must be derived from animal data [30]. Due to the surface area limitation, coated MNs have been used primarily for potent or low-dose therapeutic agents, such as vaccines, for which they have been shown to induce similar or better immune responses

Fig. 1 Microneedle application, delivery of therapeutics, and consumed microneedle by type: **a** solid microneedles are used to generate transient pores in the stratum corneum, and after microneedle removal, drug is applied to permeate through the pores; **b** hollow microneedles are used similarly to hypodermic needles, providing solid temporary channels through the stratum corneum for transdermal delivery; **c** dissolving microneedles are embedded in the skin to release drug, with only the backing remaining after use; **d** coated microneedles use solid microneedles as a carrier to implant the coating in the skin, after which the carrier microneedles are removed; **e** swellable microneedles penetrate the skin and absorb interstitial fluid, which causes the microneedles to swell and then act as conduits for drug delivery



compared to conventional hypodermic needle-based injections [24]. Because the therapeutic is in the solid state, coated MNs generally provide improved stability over conventional products [58, 59]. Swellable MNs also offer flexibility in drug loading when combined with a reservoir, such as a drug-loaded adhesive patch [53, 60] or lyophilized drug wafer [52], and have been demonstrated to deliver a range of molecules (171–67,000 Da) through the swollen hydrogel matrix [53]. By controlling the density of crosslinking, the hydrogel network acts as a rate-controlling membrane for water uptake and thus sustained drug release [52], and because swellable MNs are removed intact from the skin after application, the risk of polymer buildup is minimized [61]. Swellable MNs, however, are limited to therapeutics that are stable to crosslinking conditions or to polymers capable of crosslinking under mild conditions.

Microneedle design considerations

Polymers offer numerous advantages in MN development due to a wide range of physicochemical and mechanical properties which can be exploited to tailor a delivery strategy for a specific therapeutic agent and vice versa [10]. The use of dissolving or biodegradable materials in MNs is ideal because the

materials can be chosen based on degradation or dissolution profiles [38, 62], processability [11], crosslinking or pore-forming capacity [63, 64], or responses to specific stimuli within the microenvironment [65]. Additionally, the risk of buildup within the skin is decreased as compared to nonbiodegradable biocompatible materials [66]. Irrespective of the design strategy, MNs must function properly to be safe and effective.

In considering universal acceptance criteria for MNs, Lutton et al. proposed three basic requirements: (1) must pierce the skin; (2) must penetrate, remain intact, or dissolve in the skin while delivering the therapeutic agent; and (3) must be able to dissolve within the specified timeframe or else be removed [29]. For dissolving MNs, drug loading can compromise the mechanical strength needed to pierce the SC [49]. Wang, Hu, and Xu added that dissolving MNs should be biocompatible without unintended immunogenicity and that fabrication techniques should be compatible with sensitive therapeutic agents [10]. According to Johnson et al., MNs constructed of biodegradable materials are ideal for patient safety because the risk of unintended MN fracture within the skin is eliminated. Through proper selection of materials by which to control drug delivery and release, the efficacy of the dissolving MN systems can be maximized and side effects minimized

Table 1 Advantages and limitations of dissolving, coated, and swellable microneedles

Microneedle type	Advantages	Limitations	References
Dissolving	<ul style="list-style-type: none"> • Flexible drug loading—throughout array or restricted to regions or microparticles • Tunable delivery rate based on choice of polymer, MN design • Lack of sharps waste 	<ul style="list-style-type: none"> • Long-term safety for repeated intradermal exposure or potential build-up of biocompatible and biodegradable materials has not been established in humans 	<ul style="list-style-type: none"> [55] [14] [49] [56] [57] [30]
Coated	<ul style="list-style-type: none"> • Improved stability in the solid state • Tunable delivery strategy based on polymer(s), architecture, and thickness of film • Reduced exposure risk per treatment compared to dissolving MNs 	<ul style="list-style-type: none"> • Drug loading on MN surface—restricted to potent or low dose therapeutic agents or vaccines • Biohazardous sharps waste after use 	<ul style="list-style-type: none"> [24] [58] [59]
Swellable	<ul style="list-style-type: none"> • Flexible drug loading—increased dose when combined with drug patch or wafer • Tunable delivery rate by controlling density of crosslinking • Range of therapies delivered through hydrogel matrix (0.17–67 kDa) • Removal of swollen MNs after use reduces risk of intradermal material accumulation 	<ul style="list-style-type: none"> • Restricted to therapeutics stable to crosslinking conditions (i.e., heat, UV exposure) or polymeric materials capable of crosslinking under mild conditions (i.e., freeze/thaw) • Biohazardous waste after use 	<ul style="list-style-type: none"> [52] [53] [60] [61]

[38]. Similarly, for safe and efficacious coated and swellable MNs, drug stability during manufacturing and the selection of materials capable of controlling release are central to the design strategy [50]. For coated MNs, the coating must be designed to withstand insertion forces to be deposited within the skin [44, 67]. Due to the inherent manipulability of polymeric materials, new technologies continue to be developed and existing technologies have been adapted specifically to exploit them. In the literature, MNs of numerous geometries [68], mechanical strengths [69], ranges of sizes [38], aspect ratios [36], interspacing [70], functionality [20, 71], and delivery strategies [49, 56, 72] have been investigated, as well as the

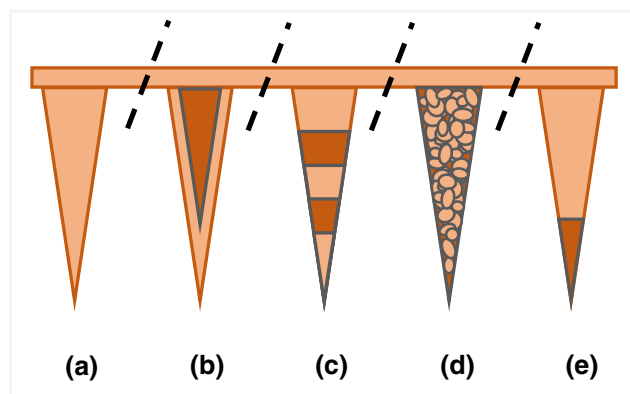


Fig. 2 Dissolving microneedle array illustrating flexibility in drug loading: **a** drug loaded homogeneously throughout a microneedle; **b** laminate layers within a microneedle; **c** horizontal layers within a microneedle; **d** drug-loaded microparticles within a microneedle; **e** drug loaded in the tip of a microneedle

pain, convenience, compliance, and safety associated with them [30].

Clinical development of microneedles

As noted by several authors, the small number of dissolving MN products in clinical development does not accurately reflect the focus, extent, and expertise dedicated to this research activity reported in the literature [19, 29]. While the majority of recently active clinical trials for non-cosmetic applications of MNs were for influenza vaccination, as of January 2017, Bhatnagar, Dave, and Venuganti noted that only hollow MN injectors have made it into clinical trials and to the market for immunization [31]. The limited information available regarding the use of a variety of MN products in humans highlights the importance of the recently published results of a phase I clinical test of dissolving MNs for influenza vaccination [9]. It is worth noting that this phase I clinical trial was preceded by a bridging study in 15 human subjects that investigated the tolerability, usability, and acceptability of a placebo dissolving MN patch [8]. Although these MN formulations comprised different materials (polyvinyl alcohol/sucrose in the bridging study versus gelatin/sucrose in the clinical study), the referenced multi-step micromolding fabrication process was the same [73].

Micromolding for microneedles

Micromolding has been widely utilized in the fabrication of dissolving MNs from biocompatible and biodegradable materials [10]. The pervasiveness of micromolding in the literature is likely due to the high reproducibility and precision [69], versatility [74], and potential cost-effectiveness [75], as well as the reusability of the molds [69]. As illustrated in Fig. 3, a typical micromolding production cycle for dissolving or swellable MNs involves three major steps: (1) fabrication of

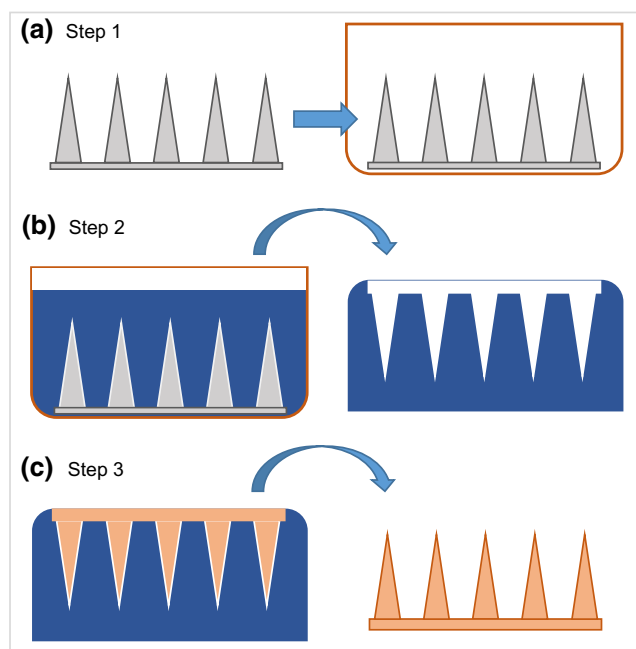


Fig. 3 The three steps in a typical micromolding production cycle: **a** in Step 1, a master mold is fabricated from a strong material (such as metal or silicon) and prepared for use as a master mold; **b** in Step 2, a negative mold is made from the master mold (usually with PDMS); **c** in Step 3, drug is loaded into the negative mold (usually in a polymer solution or melt) to create the final microneedles of the same shape and dimensions as the master mold

master molds from a strong material (i.e., metal or silicon) with preparation for use as a master mold; (2) fabrication of negative molds (typically from polydimethylsiloxane or PDMS) from the master mold; and (3) formation of the final MN structure within the negative mold. Each of these three steps could involve multiple other steps. For example, insufficient wetting of the PDMS mold due to high surface tension of aqueous formulations [14] or premature cooling due to high viscosity of thermoplastic polymers [74] can result in unwanted air trapped in the mold, which has led to the incorporation of a centrifugation or vacuum-filling step in many micromolding processes [11, 13, 76]. Myriad variations of micromolding have been discussed in the literature, with significant effort focused on the third stage of production and involving novel means of filling or forming MNs in the molds.

Adjustments have been made to micromolding conditions to improve compatibility with sensitive compounds and to enhance delivery strategies through heterogeneous filling of the molds. In-mold UV photopolymerization at room temperature [48] and vacuum loading with low heat dehydration [13] were used to fabricate dissolving MNs for the delivery of a temperature-sensitive model protein (β -galactosidase enzyme). In-mold hydrogel crosslinking by cryo-gelation (or phase transition crosslinking) was used as a low-temperature fabrication technique for swellable MNs [69, 77]. Hydrogel microparticles were loaded within a polymer matrix to

fabricate swelling triggered MNs [78], whereas sequential microparticle filling and melting steps were used to micromold layered or arrowhead dissolving MNs [74]. Microparticles were loaded into molds and fused by ultrasonic welding to create porous MNs, but at 75% porosity, these structures did not have sufficient mechanical strength to pierce skin [74]. By modifying polymer concentration to control solution viscosity, bubble MNs were fabricated using one- or two-step micromolding processes. This intentional under-filling of the MN molds effectively isolated drug to the needle tips [56, 79].

Improvements in manufacturing techniques

Despite the potential cost-effectiveness associated with micromolding [19], the multi-step batch processes are not continuous manufacturing techniques and would therefore require multiple unit operations to be scaled for translation to high throughput manufacturing [35]. While MEMS processes originated in high throughput manufacturing of microstructures [75], the expense associated with direct manufacture of MNs using MEMS eclipses that of micromolding [80], and therefore, new manufacturing techniques are warranted. There are notable recent improvements in MN manufacturing methods and technology aimed at closing the gap between efficient fabrication processes and cost-effective scalability. Table 2 summarizes some of the key processing considerations, improvements over conventional fabrication processes, and considerations for scale-up for the highlighted fabrication techniques.

Micromilling to make master molds

In an effort to facilitate timely design optimizations for dissolving MNs, Bediz et al. used micromilling to fabricate master molds from poly(methyl methacrylate) (PMMA), which were subsequently employed in the conventional three-stage micromolding production cycle outlined above [20]. This mechanical micromilling process used ultrahigh speed, high precision, rotating single-crystal diamond tools to cut a MN design out of a substrate as shown in Fig. 4 and accurately produced a series of master molds for MN arrays within minutes to hours. With this technique, master molds can be milled out of PMMA, poly(lactic-co-glycolic acid) (PLGA), metal, or ceramic, though PMMA was selected for its strength, machinability, and wear resistance. PMMA MN templates were manufactured in several geometries including square pyramidal, obelisk, and tapered obelisk, with fillets. Different cutting tools (i.e., with a tapered, straight, or negative tapered cutting edge) were utilized for different MN designs, and more than one was needed to create the obelisk geometries [20].

Table 2 Selected microneedle fabrication techniques

Technique	Materials cited	Key processing considerations	Improvements over conventional	Considerations for scale-up	Ref.
Micromilling	PMMA, PLGA, metals, ceramics	Micromolding-based—precludes geometries like overhanging structures; multiple cutting tools required	Rapid prototyping supports optimization; can use different materials	Custom-built system; expensive single-crystal diamond tools	[20] [32] [69]
Atomized spraying to fill molds	Trehalose, fructose, raffinose, PVA, PVP, CMC (with glycerol), HPMC, sodium alginate	Viscosity of 1 and 22 mPa·s and 5% w/v solutions used; amorphous MNs formed; material influenced skin penetration	No heat required; viscosity-independent; horizontal or laminate layered-MNs can be fabricated	Amenable to continuous processing	[14]
Inkjet printing to fill molds	Trehalose, PVA, polysorbate 80; trehalose MNs with or without PVA and influenza vaccine	1–70 pL droplets; viscosity, surface tension, and nozzle backpressure affect droplet formation; high shear within the nozzle	Targeted dispensing reduces material loss; without wetting agents; bilayered MNs can be fabricated	Amenable to continuous processing	[33]
Droplet-born air blowing	Dye in CMC, HA, or PVP; insulin-loaded CMC	Dose determined by concentration and droplet volume; minimal design flexibility	Micromold-free; no heat or UV irradiation; ≤ 10 min/patch	Mold-free fabrication; batch processing	[34]
Electro-drawing	PLGA in dimethyl carbonate and rhodamine 6G, Nile red, or rhodamine-labeled human serum albumin	MNs on flexible substrate or holder; minimal design flexibility	Micromold-free; nozzle-free; non-contact; low heat (20–40 °C)	Potential for continuous processing	[35]
Drawing lithography	SU-8; maltose with vitamin C or B3	Heat required; glass transition determines manufacturing properties; minimal design flexibility	Micromold-free; ultrahigh aspect ratio MNs	Mold-free fabrication; batch processing	[36]
3D printing	A proprietary resin, 3DM-Castable	UV irradiation; 50 μm XY resolution; MN width deviated from design; topical application of drug	Rapid prototyping of a personalized solid MN splint for a patient's finger	Point-of-care; no mass production	[37]
Continuous liquid interface production	TMPTA, PAA, and photopolymerizable derivatives of PEG and PCL; PAA, PCL, and PEG with rhodamine B	UV irradiation; use “working curve” to translate designs to different resins	Oxygen-permeable window eliminates repositioning steps, improves accuracy; ≤ 10 min/patch	Continuous production	[38]
Inkjet printing to coat MNs	Quantum dots coated on PMVE/MA MN; PGA MN coated with PMVE/MA release layer, then itraconazole; SS MN coated with 5-FU, curcumin, or cisplatin in Soluplus; SS MN coated with insulin in gelatin, trehalose, Soluplus, or POX	Aqueous solutions, colloids, and some organic solvents; droplet formation depends on nozzle size (300 pL), applied voltage, and frequency or duration of pulse	Non-contact dispensing of uniform, precise, and accurate coating layers; reduced material loss; without wetting agents	Rapid processing times; ease of scalability	[39] [41] [4-0] [82] [87] [88]
Poly-electrolyte multilayers to coat MNs	Plasmid DNA/poly-1 coated SS MN; ICMVs/poly-1 with fluorescent ovalbumin coated PLGA MN; PLLA MN coated with release layer, then multilayers including plasmid DNA/poly-1	Layer by layer assembly of ultrathin, uniform coatings; high weight fractions of therapeutics; tailor release profile with polymer or film structure, i.e., rapid, sustained, or multi-therapeutic release	Design films that rapidly deposit into skin for sustained release of therapeutics; lipid nanocapsules showed improved protein subunit vaccination	Convert to spray or inkjet deposition; may still require batch processing	[42] [43] [44] [90]

Precise alignment steps for re-tooling require the assistance of a microscope. Additionally, the custom-fabricated single-crystal diamond cutting tools and the micromilling system are custom-made, adding to the overall expense of this technique. Combined with finite element analysis, effective design changes can be realized with micromilling, as shown by Bediz et al. [20]. However, to maximize the potential of this

design flexibility in a high throughput manufacturing environment, considerations must be made to ensure quick, consistent, and accurate re-tooling and alignment steps. Minimizing the use of design-specific cutting tools could streamline and simplify design changes. Regardless of the tooling used for micromilling the master molds, the limitations of micromolding would still apply to manufacturing the actual

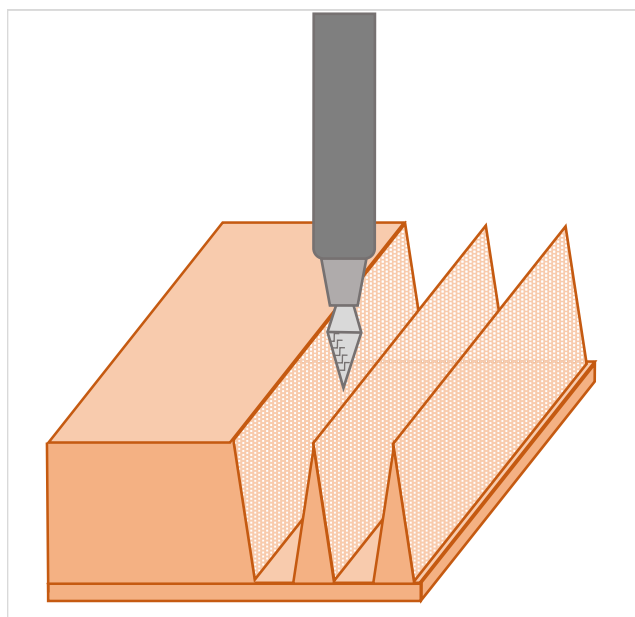


Fig. 4 Micromilling to produce master molds uses ultrahigh speed, high precision, rotating single-crystal diamond cutting tools to machine microneedle designs out of a hard substrate such as PMMA (or PLGA, metal, or ceramic) within minutes to hours

MNs, including difficult translation and scalability of the multi-step batch processing to high throughput manufacturing.

Atomized spraying to fill molds

Eliminating the need for a centrifugation or vacuuming step from a micromolding process could significantly improve the translation to continuous manufacturing, which is readily scalable [81]. An alternative means to eliminate unwanted air pockets trapped in molds due to high aqueous surface tension, as mentioned above, involves improved dispensing into micromolds, as illustrated in Fig. 5. Removing trapped air improves the accuracy and precision of the MN manufacturing process and could also reduce mechanical failures due to voids within individual MNs. McGrath et al. hypothesized that atomization of aqueous solutions from a nozzle could disrupt cohesive forces and wet the MN mold surface and voids [14]. They demonstrated this by fabricating dissolving MNs with atomized spraying at room temperature into PDMS micromolds using a two-fluid external mixing nozzle capable of producing 10–50- μm droplets with a 0.25-bar compressed air feed and a 1.5-mL/min aqueous feed of 5% *w/v* solids dissolved in deionized water. Several materials were investigated including trehalose, fructose, raffinose, polyvinyl alcohol (PVA), polyvinylpyrrolidone (PVP), carboxymethyl cellulose (CMC) with glycerol, hydroxypropyl methylcellulose (HPMC), and sodium alginate (at 0.35% *w/v*).

Although the viscosity of the materials in solution varied between 1 and 22 mPa·s, changes in viscosity did not prevent

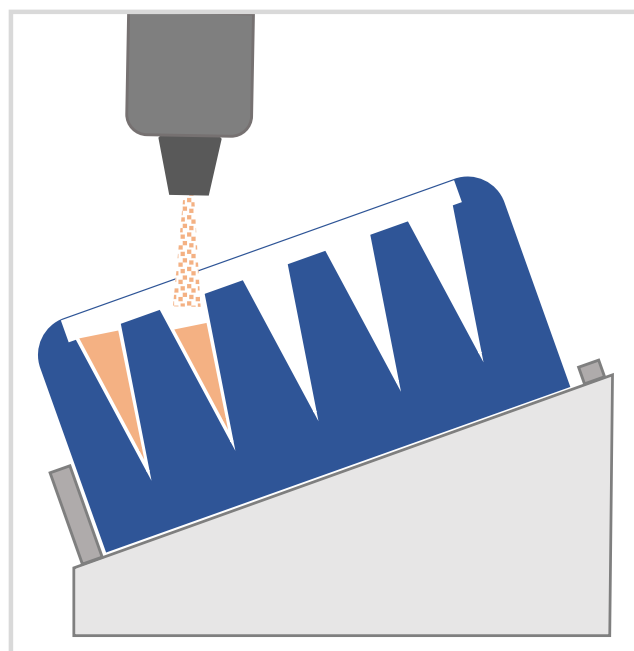


Fig. 5 More recently utilized dispensing methods for micromold filling such as atomized spraying or inkjet printing eliminate the need for a separate centrifugation or vacuuming step to remove trapped air from the molds, thereby improving not only the accuracy and precision of the microneedle manufacturing process, but also the translation to continuous manufacturing, which is readily scalable

sufficient mold-filling by this atomized spraying process. The MN material did however significantly affect the physical penetration of the skin, with the highest frequencies of full epidermal breach measured for trehalose and fructose MNs. Single-component MNs were determined to have amorphous compositions, which could theoretically improve protein stability. Multicomponent MNs were fabricated in horizontal or laminate layers, showing some design flexibility but at the expense of extra processing steps. Overall, this micromolding technique is amenable to continuous manufacturing under mild processing conditions and could be useful for active ingredients that are sensitive to high temperature, viscosity, or concentration [14]. The major hurdles for scaling up production of MNs made with this process include sterilization and potential safety issues related to the use and repeated application of non-therapeutic materials that would dissolve and possibly buildup, within the skin.

Inkjet printing to fill molds

Another mold-filling technique amenable to continuous manufacturing involves inkjet printing into molds. In piezoelectric drop-on-demand (DOD) inkjet printing, an applied voltage and frequency deform a piezoelectric ceramic element to eject picoliter droplets, and therefore, inertia, solution viscosity, and surface tension are critical parameters for this technique [82]. Allen et al. performed initial screening

experiments of 30–50% *w/v* trehalose, 0–2.5% *w/v* PVA, and 0–0.10% *w/v* Tween 80 aqueous solutions to determine the optimal formulation for piezoelectric printing and PDMS mold wetting based on the *Z* values calculated from the screening results [33]. PVA was shown to increase surface tension and decrease viscosity and contact angle, leading to better droplet formation and wetting of the mold, whereas the surfactant Tween did not significantly effect contact angle and therefore did not improve wetting.

The customized printer used in these experiments was equipped with an 80- μm diameter orifice, a 5-mL syringe reservoir, and a bipolar trapezoidal waveform. Backpressure within the jet reservoir was set manually, with a low range of 2–4 mbar and a high range of 8–12 mbar, voltage was varied between 25 and 80 V, and frequency was varied from 50 to 16,000 Hz. Despite screening results and droplet tests indicating that 30% *w/v* trehalose without PVA produced unsuitable droplets for micromold filling, Allen et al. successfully fabricated MNs by inkjet printing trehalose with and without PVA. By applying a low backpressure and at least 50 V, the formulation without PVA and having an unfavorable *Z* value (> 20) was successfully used to print MNs, thereby overcoming the droplet formation limitations predicted by the *Z* value and demonstrating the importance of actuation parameters for this technique [33].

Piezoelectric DOD printing is a high shear process that creates high surface-to-volume droplets in the 1–70 pL range with a high precision ($< 5\%$ RSD) [33, 82]. To demonstrate the precision and accuracy of the dispensing process for MNs, Allen et al. printed bilayer MNs with 25 or 100 drops of formulation containing Congo red for direct observation of the layers. To characterize the physical effects of this high shear dispensing on vaccine stability, an inactivated trivalent influenza vaccine in 30% *w/v* trehalose with 1% *w/v* PVA was analyzed by single radial immunodiffusion (SRID) assay before and after dispensing at different piezo voltages and frequencies. Results indicated that higher voltages (≥ 50 V) were

problematic, but vaccine integrity was maintained at 30 V and 50–16,000 Hz [33].

Piezoelectric inkjet dispensing enables micromolding with precise dosing and could be useful for potent or expensive therapeutics, in a readily scalable format. Similarly to atomized spraying to fill molds, this micromold filling technique is amenable to continuous manufacturing, though actuation parameters for the piezo must be selected carefully to achieve suitable drop formation as well as to maintain stability of the therapeutic agent. Again, major hurdles for scale-up include sterilization and potential safety issues related to the use of non-therapeutic materials that would dissolve and possibly persist in the skin.

Surface drawing to form MNs

Droplet-born air blowing (DAB) [34], electro-drawing [35], and drawing lithography [36] are direct MN fabrication techniques that rely on surface properties and are micromold-independent. Freedom from the mold necessitates that other forces govern the shape of the MN formation, with aspect ratio (AR, as height over width) essentially being the only adjustable geometry for these techniques.

DAB is the mildest of the three processes, with room temperature fabrication in under 10 min, and also requires minimal equipment [34]. As depicted in Fig. 6, droplets are dispensed onto plates (Fig. 6(a)), two plates are stacked facing each other such that droplets touch (Fig. 6(b)), and the subsequent separation of the plates with the application of air (Fig. 6(c)) results in an array of MNs on each plate (Fig. 6(d)). The utility of DAB was demonstrated by fabricating CMC, hyaluronic acid (HA), or PVP MNs with dye at different lengths and measuring the axial fracture force of the MNs. CMC MNs were the strongest, and therefore, an insulin-loaded version of these MNs was fabricated. These MNs achieved bioavailability comparable to subcutaneous

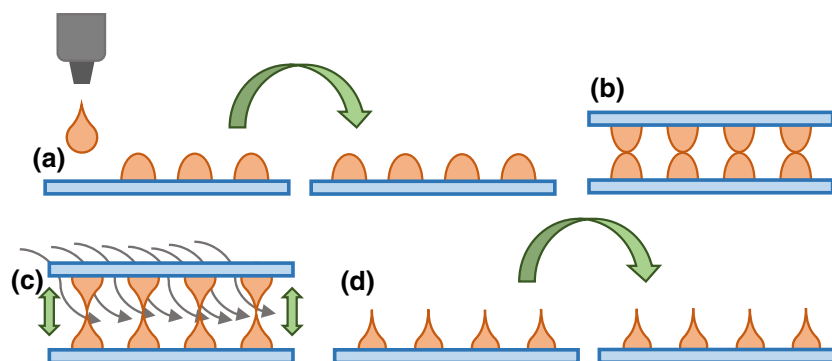


Fig. 6 Droplet-born air blowing is a micromold-free manufacturing process for making microneedles at room temperature in under 10 min using four steps: **a** droplets are dispensed onto plates, **b** two plates are stacked facing each other such that the droplets touch, **c** a stream of air is directed

between the plates as they are separated, forming elongated microneedle structures, and **d** the microneedles are separated, with the formation of a microneedle array on each plate

injection of the same insulin formulation and glucose down-regulation in diabetic mice [34].

Electro-drawing enables contact-free fabrication at 20–40 °C by heating a polar dielectric crystal such as lithium tantalate at a fixed distance from droplets on a surface, which can be flexible [35]. Droplets are dispensed on a surface (Fig. 7(a)), then drawn into MNs through the application of an electro-hydrodynamic force (Fig. 7(b)), then subsequently solidified upon solvent evaporation with optional heat treatment (10 min at 40 °C) to sharpen tips (Fig. 7(c)). MNs were prepared from PLGA in dimethyl carbonate with rhodamine 6G, Nile red, or rhodamine-labeled human serum albumin for visualization [35].

Maltose MNs with and without ascorbic acid-2-glucoside (1% w/w) and niacinamide (1.5% w/w) were fabricated using drawing lithography [36]. Maltose is a liquid above its 102–103 °C melting temperature and when cooled exhibits a quick increase in viscosity over its narrow 95 ± 4 °C glass transition temperature range [36]. The viscosity in the glassy state is the critical parameter that must be controlled for manufacturing performance. As seen in Fig. 8, to make MNs by drawing lithography, maltose was melted onto a plate, and an array of pillars attached to a drawing plate was lowered into the melt. The drawing plate was drawn up out of the melt at a controlled speed and therefore controlled rate of cooling, in steps, such that maltose was elongated into MN structures. Ultrahigh aspect ratio (UHAR) MNs (AR > 100) can be formed with this type of drawing lithography [36].

While these three drawing techniques are performed without micromolds, scale-up would still likely entail batch processing to accommodate the formation steps. DAB would best suit thermally labile therapeutics, while drawing lithography would better suit thermally stable drugs, possibly those intended to penetrate to the highly vascularized lower dermis by way of UHAR. Electro-drawing might be suitable for a continuous process or in a personalized medicine or point-

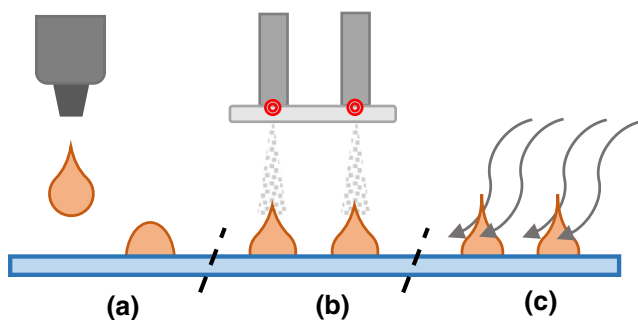


Fig. 7 Electro-drawing is a micromold-free manufacturing process for making microneedles at 20–40 °C using three steps: **a** droplets are dispensed onto a surface; **b** a polar dielectric crystal (i.e., lithium tantalate, LiTaO₃, a pyroelectric crystalline solid) is heated at a fixed distance from the droplets, resulting in an electro-hydrodynamic force that draws the droplets into microneedle shapes; **c** the microneedles solidify upon solvent evaporation with optional heat treatment (10 min at 40 °C) to sharpen the tips

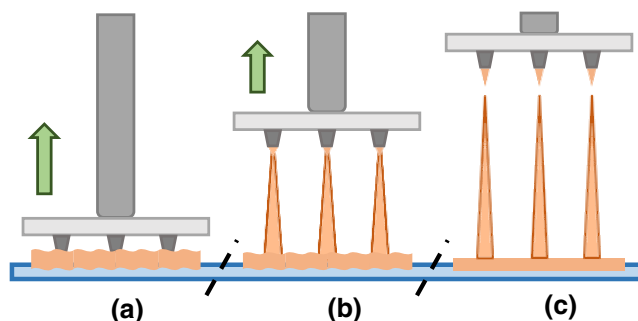


Fig. 8 Drawing lithography is a micromold-free manufacturing process that utilizes the glassy state of thermoplastic materials such as maltose for making microneedles in three major steps: **a** maltose is melted onto a plate, and an array of pillars attached to another plate is lowered into the melt; **b** by drawing the top plate out of the melt at a controlled speed, which imparts a controlled rate of cooling, the maltose is drawn in its glassy state into elongated structures attached to the pillars; and **c** the microneedles are detached from the pillars

of-care mode. Major regulatory hurdles for all three techniques include sterilization or aseptic processing, which might require the use of laminar airflow hoods or cleanrooms due to the level of exposure of the MNs to the environment and the higher associated risk for contamination. The safety issues mentioned previously related to the use of dissolving MNs and material accumulation within the skin would also apply to these MNs. While maltose has been shown to dissolve in the skin and therefore could present less of a concern regarding accumulation [36], potential interference with the intended application (i.e., insulin delivery) or auxiliary diagnostics (i.e.; blood glucose monitoring test strips) would need to be investigated to justify the choice of this material [83].

Photostereolithography to form MNs

Stereolithography is a scalable, additive manufacturing technique in which a structure is fabricated out of successive layers of resin, with the shape of each layer dictated by a mask or a digital light processor (DLP), through which UV light is guided for polymerization [84]. Lim, Ng, and Kang used a bottom-up DLP stereolithography instrument to 3D-print customized finger splints with a bed of MNs on the inner surface [37]. They utilized a proprietary resin (3DM-Castable) and an XY resolution of 50 μm for printing and were able to achieve MNs having ~1.4 AR and tips as small as ~50 μm. The overall strategy was to print a personalized splint for immobilization of the finger with simultaneous penetration of the SC by the MNs for permeation by a topical non-steroidal anti-inflammatory drug (NSAID) [37]. While the MNs were designed to have a base of 300 μm, a height of 900 μm, and interspacing of 1800 μm center-to-center, the actual printed MNs on the splint had a base of ~600 μm, a height of ~800 μm, and the correct interspacing. The deviation in base diameter from design was attributed to the known limitation of this printing process, which is associated with separation and

alignment steps between each printed layer and the resin container [37, 38].

Continuous liquid interface production (CLIP) is an additive manufacturing technique that differs from conventional photostereolithography by integrating an oxygen-permeable window at the UV light/resin interface to prevent unwanted polymerization (see Fig. 9(a)), thereby improving process efficiency [38]. Figure 9(b) shows the same photolithography setup but without the oxygen-permeable window, illustrating the uninhibited polymerization between the object and the UV light/resin interface, as would have occurred in the 3D printing process reported by Lim, Ng, and Kang [37]. Johnson et al. demonstrated the utility of CLIP by fabricating square pyramidal, arrowhead, tiered, and turret MNs from trimethylolpropane triacrylate (TMPTA), a model resin chosen for the ideal processing characteristics of fast photopolymerization and low viscosity. Because light intensity and build speed are critical polymer-dependent processing parameters, a “working curve” was created to assist in normalizing differences in reaction kinetics between the various materials used in these CLIP studies. Construction of the curve enabled the TMPTA build parameters to be adapted to make biocompatible MNs from poly(acrylic acid) (PAA) and methacrylate functionalized poly(caprolactone) (PCL) and swellable hydrogel MNs from methacrylate functionalized poly(ethylene glycol) (PEG) [38]. The light intensity used to manufacture TMPTA MNs varied from 1.35–5.4 mW/cm² UV light, while intensities of 1.2–8.9 mW/cm² UV light were used to make biocompatible MNs. Build speeds varied between 25 and 100 mm/h with all patches produced in under 10 min/patch using CLIP.

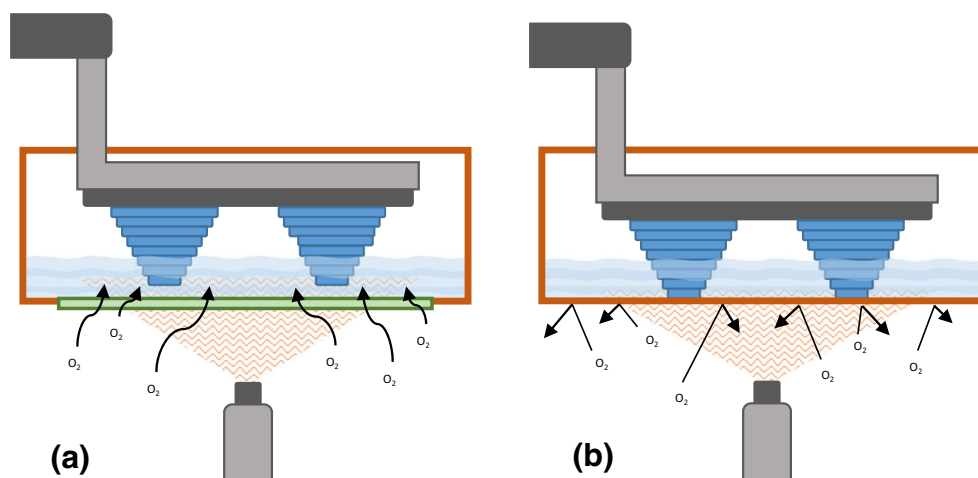


Fig. 9 Continuous liquid interface production is a micromold-free photostereolithographic process for making microneedles in under 10 min/array that utilizes an oxygen-permeable window at the UV light/resin interface for improved efficiency and accuracy: in **a**, the use of an oxygen-permeable window inhibits polymerization of the microneedle construct on the interface, eliminating the need for

Both of these additive manufacturing techniques rely on UV exposure and are therefore unsuitable for direct incorporation of therapeutics that photodegrade at the polymerization wavelengths. Additionally, unpolymerized monomer and/or residual solvents used in washing steps could present an issue if toxic or lacking biocompatibility. Unlike CLIP, which is a readily scalable technique, the 3D-printed finger splint would be a personalized device dependent upon obtaining user data and conversion to a 3D-printable file and perhaps printed and dispensed only once or a few times at a local pharmacy. The widespread use of this point-of-care printing technology could be significantly restricted by equipment costs, technological training requirements, and lack of familiarity to prescribing physicians and insurance drug formularies. Regulatory hurdles for both techniques include sterilization, though UV light itself or in combination with a gas, could prove useful for sterilizing the MNs and could possibly replace the UV post-curing step reported for both techniques [85, 86].

Inkjet printing to coat MNs

As mentioned above, inkjet printing is a readily scalable format with high precision and accuracy capabilities. With picoliter droplet volumes and compatibility with aqueous solutions and some organic solvents, this technology is a logical choice for MN coating, with successful printing of a variety of molecules demonstrated in the literature [82, 87]. Boehm et al. used piezoelectric DOD inkjet printing to coat poly(methylvinylether/maleic anhydride) (PMVE/MA) MNs with quantum dots [88]. A phosphate-buffered saline/borate buffer containing these 2–10-nm nanocrystals

separation and alignment steps; in **b**, an equivalent bottom-up setup using a conventional process without the oxygen-permeable window shows the uninhibited polymerization between the microneedle construct and the UV light/resin interface, necessitating separation and alignment steps which could lead to deviations from design dimensions

was filled into a 1.5-mL reservoir and printed onto MNs through a single 21.5- μm nozzle in a triangular pattern ten layers thick. Though scanning electron micrographs (SEM) showed evidence of hydrolysis and buffer crystallization on coated MN surfaces, the MNs (500 μm width and 1000 μm height) were used to deliver quantum dots to a depth of ~ 200 μm in porcine skin within 1 h. In another study, Boehm et al. coated polyglycolic acid (PGA) MNs with multiple components, using optimized printing parameters including droplet velocity, cartridge temperature, drop spacing, droplet count, and firing frequency [41]. Ten layers of a PMVE/MA in dimethylsulfoxide (DMSO) solution were applied to the MNs to provide a water-soluble release layer, followed by 20 layers of itraconazole, a hydrophobic antifungal, in a coconut oil-benzyl alcohol carrier (with and without methylene blue for visualization). SEM showed coated and uncoated MNs, and optical micrographs showed release within 3 h in porcine skin of methylene blue dye in the itraconazole layer [41].

In another 3D-printing study, layers of insulin in aqueous solutions of gelatin, trehalose, Soluplus (co-polymer of polyvinyl caprolactam–PVA–PEG), or poly(2-ethyl-2-oxazoline) (POX) were printed onto stainless steel (SS) MNs by Ross et al., with only Soluplus providing an acceptable in vitro release of 95% at 30 min [39]. The insulin/polymer solutions were printed in sequences of six 300 pL droplets over 50 cycles with optimized piezoelectric parameters including a nozzle speed of 1–5 m/s, 100 V applied voltage, and 60 μs pulse duration. Uddin et al. studied inkjet printing onto SS MNs of ethanol or aqueous solutions of 3–9% w/v Soluplus containing 3% w/v 5-fluorouracil, curcumin, cisplatin, or sodium fluorescein [40]. They reported the critical parameters for coating

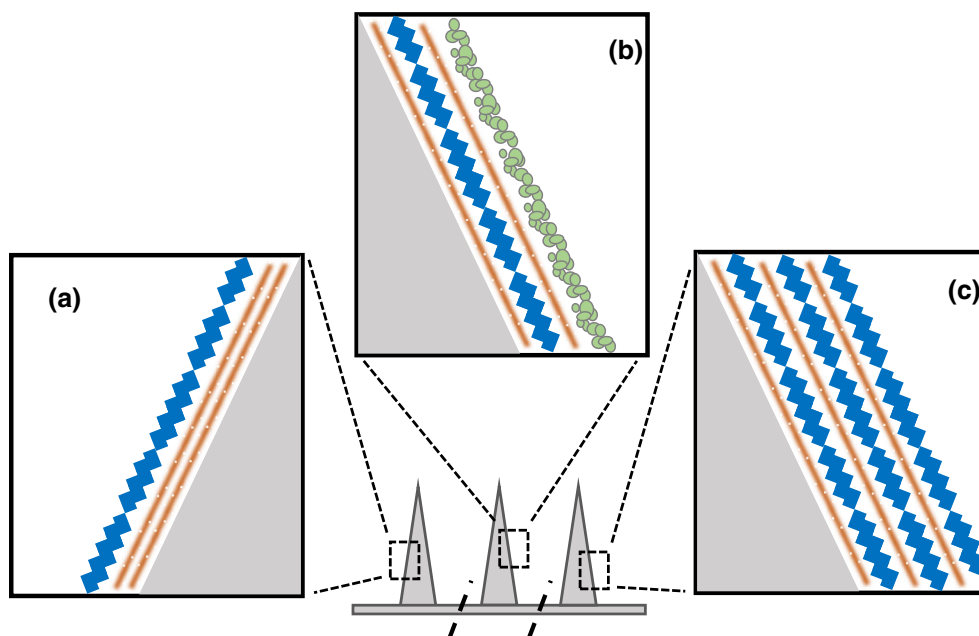
deposition to be nozzle size, applied voltage, and pulse duration. The viscosities of the coating solutions ranged from 36 to 67 cP, which did not clog the 300-pL volume nozzle, but they implemented a preventive washing step using ethanol or water as a precaution. The optimized parameters in this study were the same as those for Ross et al. [39, 40].

With clear advantages over conventional multi-step dip coating processes including accuracy, reproducibility, reduced waste, and scalability, coating by inkjet printing is primarily limited by the available MN surface area that can be directly targeted for printing (i.e., planar surfaces) and is therefore most useful for potent therapeutic agents [88]. As noted above, inkjet printing techniques are amenable to continuous manufacturing. Printing parameters and nozzle size must be considered to effectively coat the MN surface and to avoid clogging the nozzle, as should the compatibility between the coating formulation and the MNs. Sterilization of the base MNs followed by aseptic processing for inkjet coating could avoid or reduce the deleterious effects noted from sterilization by gamma irradiation or heat treatments [89].

Polyelectrolyte multilayers (PEMs) to coat MNs

PEMs are ultrathin films fabricated by alternating adsorption of charged polymers and therapeutic materials such as proteins, DNA, or nanoparticles (NP) on a substrate to achieve a high weight fraction of the active [44]. PEM-coated MNs are designed such that the release characteristics of the film are determined by choice of materials, film thickness, and overall structure (i.e., by use of release layers (Fig. 10(a)), by coating with multiple components (Fig. 10(b)) or use of nested sequential layers (Fig. 10(c)). Saurer et al. prepared PEMs from

Fig. 10 PEMs are ultrathin film coatings that are constructed on microneedles by alternating adsorption of charged polymers and high weight fractions of therapeutic materials (i.e., proteins, DNA, or nanoparticles) and have tunable release profiles based on the choice of materials, film thickness, and overall structure which is illustrated for microneedles designed with **a** a release layer (i.e., pH sensitive for immediate release), **b** multiple components, or **c** nested sequential layers



plasmid DNA with a poly(β -amino ester) (poly-1) on SS MNs [42], whereas DeMuth et al. prepared them from sequential layers of lipid-coated PLGA nanoparticles (NP) with poly-1 and firefly luciferase with poly-1 on the same PLGA MNs [90]. Then, DeMuth et al. prepared PEMs on PLGA MNs from poly-1 and interbilayer-cross-linked multilamellar lipid vesicles (ICMVs) carrying the molecular adjuvant monophosphoryl lipid A and a protein antigen [43]. These MNs were shown to deposit the PEMs in the skin, with sustained release of ICMVs for 24 h in vivo. Rapid pH-sensitive transfer into the skin followed by sustained release of days to weeks was achieved for PEM-coated poly(L-lactide) (PLLA) MNs carrying a DNA vaccine along with molecular adjuvants and transfection agents [44]. This study demonstrated the highly tunable nature of this “multilayer tattooing” approach, particularly regarding DNA vaccine delivery.

Despite the inherent multi-step nature of the PEM-coating process, through careful selection of solutions and equipment parameters, inkjet printing or spray deposition could likely aid in translating this technology to high throughput manufacturing. Though the same safety concerns for potential polymer buildup within the skin apply for PEM-coated MNs as for dissolving MNs, the total amount of material deposited in the skin is lower and therefore could decrease the risk of toxicity, irritation, and accumulation. Further, sterilization of the base MNs prior to coating could enable the effective use of lower doses/less destructive types of sterilization.

Further improvement of existing technologies

Other existing pharmaceutical manufacturing processes could be developed into suitable techniques for MN fabrication. Hot-melt extrusion and 3D printing by fused deposition modeling are useful techniques for continuous processing of biocompatible/biodegradable materials that could potentially be used in tandem to fabricate MN arrays directly or to make master molds for micromolding [91]. Precision extruding deposition, which is nearly a hybrid of the two techniques, could also be considered [92]. Another more recently described manufacturing technique that could potentially be used to fabricate master molds in fewer steps than MEMs is reaction-diffusion-mediated photolithography (RDP). RDP was used to fabricate arrays out of various polymers, including TMPTA, of MN-like structures with aspect ratios in the range of 1 to 3 and diameters of 20 to 200 μm [93]. This technique results in polymerization of microprojections in a single step, using collimated UV light, a simple photomask, and an oxygen-permeable (PDMS) layer. While RDP appears to overcome some of the challenges for achieving fine resolution with high precision, the scalability of this technique is undetermined and like all photolithography techniques, limited to photopolymerizable materials. To be viable for large-scale manufacture of MNs, further improvement of existing

technologies must ensure (1) the capability to achieve low-to-mid micron scale resolution (~ 25 – $100 \mu\text{m}$) with high accuracy and precision ($\sim 5\%$ or less), (2) automated processes requiring minimal or no manual operations or handling, and (3) flexibility within the fabrication technique to accommodate a variety of materials and therapeutics.

Regulatory considerations for MNs

Despite the numerous applications of MNs reported in the literature in animal studies and human assessments (primarily regarding safety or pain), no reports of infection were found [7, 8, 94–98]. The skin has been shown to recover barrier properties readily after MN treatment [94] and to be less vulnerable to *Escherichia coli* penetration than skin that was pierced by 26- and 23-gauge hypodermic needles [99]. But because MNs puncture the SC, which serves as the foremost barrier for skin protection, it is paramount to investigate the potential risk of infection presented by microbial loads introduced in the manufacturing process. Based on risk assessment, regulatory agencies may stipulate stringent microbial limits or sterility testing, depending on whether sterility is required. Whether MNs are manufactured under aseptic conditions or sterilized terminally may depend on (lack of) compatibility between terminal sterilization techniques and robust MN products [89], due to the high costs associated with sterile processing. The overall manufacturing process could be designed to utilize in-process cleaning, filtration, or sterilization steps that help to achieve or maintain low bioburdens for the MNs in downstream processes, such as sterile filtering inkjet printer ink and photopolymer solutions before use or steam sterilizing base MNs before coating. Additionally, manufacture of MNs from materials shown to have antibacterial properties may justify not needing sterilization for MN products [100].

While some studies in animals and humans have assessed the level of irritation induced by MN application [25, 101], the risk of irritation, buildup, and toxicity within the skin has not been fully characterized for use of biocompatible and biodegradable materials commonly employed in MN manufacturing. This safety concern is particularly important for dissolving MNs intended for repeated use, such as in insulin therapy. Dissolved and fractured MN materials and their impurities, degradants, and metabolites will eventually need to be investigated for irritation, toxicity, and rates of clearance to determine safety margins and to assist in determining exposure limits [102].

Other regulatory hurdles include the establishment of appropriate quality control tests and specifications, in compliance with current Good Manufacturing Practices (cGMP), to ultimately ensure the safety and efficacy of MN products. Lutton et al. suggested that the ICH guidelines for new drug products (Q6A) could be adapted for this purpose [29]. Based

on these guidelines, the tests relevant to dissolving, coated, and swellable MNs might include dissolution, disintegration (i.e., for rapidly dissolving MNs), hardness/friability (i.e., for swellable MNs), uniformity of dosage form, water content, pH, microbial limits, sterility, endotoxins/pyrogens, extractables (i.e., the base MNs for coated MNs or MN backing or adhesive), and functionality testing of delivery systems (i.e., insertion and fracture forces). A variety of analytical methods used to characterize the mechanical performance of MNs have been reported throughout the literature [70, 103, 104] and with proper justification and validation could be adopted to demonstrate compliance with cGMPs in the manufacture of MNs.

Conclusion

Biocompatible and biodegradable material-based dissolving, coated, and swellable MNs have the potential to deliver a range of therapeutics transcutaneously, and therefore, the data from the recent phase I clinical trial using dissolving MNs are exciting. Further testing in the clinic and a clear path to regulatory approval including the establishment of a guideline for appropriate quality controls is needed in order for MNs to reach their full potential as drug delivery modalities. More importantly, new techniques or improvements to existing technologies are needed for efficient and scalable manufacture of those MNs.

Compliance with ethical standards Information was gathered in compliance with current laws.

Conflict of interest The authors declare that they have no conflict of interest.

References

1. Trommer H, Neubert RH. Overcoming the stratum corneum: the modulation of skin penetration. *A Rev Skin Pharmacol Physiol*. 2006;19(2):106–21. <https://doi.org/10.1159/000091978>.
2. Alexander A, Dwivedi S, Ajazuddin GTK, Saraf S, Saraf S, et al. Approaches for breaking the barriers of drug permeation through transdermal drug delivery. *J Control Release*. 2012;164(1):26–40. <https://doi.org/10.1016/j.jconrel.2012.09.017>.
3. Brown MB, Martin GP, Jones SA, Akomeah FK. Dermal and transdermal drug delivery systems: current and future prospects. *Drug Deliv*. 2006;13(3):175–87. <https://doi.org/10.1080/10717540500455975>.
4. Walters KA. Drug delivery: topical and transdermal routes. *Encyclopedia of pharmaceutical science and technology*, Fourth Edition. CRC Press; 2013. p. 1211–23.
5. Henry S, McAllister DV, Allen MG, Prausnitz MR. Microfabricated microneedles: a novel approach to transdermal drug delivery. *J Pharm Sci*. 1998;87(8):922–5. <https://doi.org/10.1021/js980042+>.
6. van der Maaden K, Jiskoot W, Bouwstra J. Microneedle technologies for (trans)dermal drug and vaccine delivery. *J Control Release*. 2012;161(2):645–55. <https://doi.org/10.1016/j.jconrel.2012.01.042>.
7. Gill HS, Denson DD, Burris BA, Prausnitz MR. Effect of microneedle design on pain in human volunteers. *Clin J Pain*. 2008;24(7):585–94. <https://doi.org/10.1097/AJP.0b013e31816778f9>.
8. Arya J, Henry S, Kalluri H, McAllister DV, Pewin WP, Prausnitz MR. Tolerability, usability and acceptability of dissolving microneedle patch administration in human subjects. *Biomaterials*. 2017;128:1–7. <https://doi.org/10.1016/j.biomaterials.2017.02.040>.
9. Roupheal NG, Paine M, Mosley R, Henry S, McAllister DV, Kalluri H, et al. The safety, immunogenicity, and acceptability of inactivated influenza vaccine delivered by microneedle patch (TIV-MNP 2015): a randomised, partly blinded, placebo-controlled, phase 1 trial. *Lancet*. 2017;390(10095):649–58. [https://doi.org/10.1016/s0140-6736\(17\)30575-5](https://doi.org/10.1016/s0140-6736(17)30575-5).
10. Wang M, Hu L, Xu C. Recent advances in the design of polymeric microneedles for transdermal drug delivery and biosensing. *Lab Chip*. 2017;17(8):1373–87. <https://doi.org/10.1039/c7lc00016b>.
11. Lee JW, Park JH, Prausnitz MR. Dissolving microneedles for transdermal drug delivery. *Biomaterials*. 2008;29(13):2113–24. <https://doi.org/10.1016/j.biomaterials.2007.12.048>.
12. Hong X, Wei L, Wu F, Wu Z, Chen L, Liu Z, et al. Dissolving and biodegradable microneedle technologies for transdermal sustained delivery of drug and vaccine. *Drug Design, Dev Ther*. 2013;7:945.
13. Martin CJ, Allender CJ, Brain KR, Morrissey A, Birchall JC. Low temperature fabrication of biodegradable sugar glass microneedles for transdermal drug delivery applications. *J Control Release*. 2012;158(1):93–101. <https://doi.org/10.1016/j.jconrel.2011.10.024>.
14. McGrath MG, Vucen S, Vrdoljak A, Kelly A, O'Mahony C, Crean AM, et al. Production of dissolvable microneedles using an atomised spray process: effect of microneedle composition on skin penetration. *Eur J Pharm Biopharm*. 2014;86(2):200–11. <https://doi.org/10.1016/j.ejpb.2013.04.023>.
15. Miyano T, Tobinaga Y, Kanno T, Matsuzaki Y, Takeda H, Wakui M, et al. Sugar micro needles as transdermic drug delivery system. *Biomed Microdevices*. 2005;7(3):185–8. <https://doi.org/10.1007/s10544-005-3024-7>.
16. Kim YC, Quan FS, Yoo DG, Compans RW, Kang SM, Prausnitz MR. Improved influenza vaccination in the skin using vaccine coated microneedles. *Vaccine*. 2009;27(49):6932–8. <https://doi.org/10.1016/j.vaccine.2009.08.108>.
17. Ma Y, Gill HS. Coating solid dispersions on microneedles via a molten dip-coating method: development and in vitro evaluation for transdermal delivery of a water-insoluble drug. *J Pharm Sci*. 2014;103(11):3621–30. <https://doi.org/10.1002/jps.24159>.
18. Gill HS, Prausnitz MR. Coating formulations for microneedles. *Pharm Res*. 2007;24(7):1369–80. <https://doi.org/10.1007/s11095-007-9286-4>.
19. Larrañeta E, Lutton REM, Woolfson AD, Donnelly RF. Microneedle arrays as transdermal and intradermal drug delivery systems: materials science, manufacture and commercial development. *Mater Sci Eng: R: Reports*. 2016;104:1–32. <https://doi.org/10.1016/j.mser.2016.03.001>.
20. Bediz B, Korkmaz E, Khilwani R, Donahue C, Erdos G, Faló LD, et al. Dissolvable microneedle arrays for intradermal delivery of biologics: fabrication and application. *Pharm Res*. 2014;31(1):117–35. <https://doi.org/10.1007/s11095-013-1137-x>.
21. Gittard SD, Ovsianikov A, Chichkov BN, Doraiswamy A, Narayan RJ. Two-photon polymerization of microneedles for transdermal drug delivery. *Expert Opin Drug Deliv*. 2010;7(4):513–33. <https://doi.org/10.1517/17425241003628171>.

22. Lee JW, Han MR, Park JH. Polymer microneedles for transdermal drug delivery. *J Drug Target*. 2013;21(3):211–23. <https://doi.org/10.3109/1061186X.2012.741136>.
23. Ita K. Transdermal delivery of drugs with microneedles: strategies and outcomes. *J Drug Deliv Sci Technol*. 2015;29:16–23. <https://doi.org/10.1016/j.jddst.2015.05.001>.
24. Tuan-Mahmood TM, McCrudden MT, Torrisi BM, McAlister E, Garland MJ, Singh TR, et al. Microneedles for intradermal and transdermal drug delivery. *Eur J Pharm Sci*. 2013;50(5):623–37. <https://doi.org/10.1016/j.ejps.2013.05.005>.
25. Kim YC, Park JH, Prausnitz MR. Microneedles for drug and vaccine delivery. *Adv Drug Deliv Rev*. 2012;64(14):1547–68. <https://doi.org/10.1016/j.addr.2012.04.005>.
26. Indermun S, Lutttge R, Choonara YE, Kumar P, du Toit LC, Modi G, et al. Current advances in the fabrication of microneedles for transdermal delivery. *J Control Release*. 2014;185:130–8. <https://doi.org/10.1016/j.jconrel.2014.04.052>.
27. Ma G, Wu C. Microneedle, bio-microneedle and bio-inspired microneedle: a review. *J Control Release*. 2017;251:11–23. <https://doi.org/10.1016/j.jconrel.2017.02.011>.
28. Rejinold NS, Shin JH, Seok HY, Kim YC. Biomedical applications of microneedles in therapeutics: recent advancements and implications in drug delivery. *Expert Opin Drug Deliv*. 2016;13(1):109–31. <https://doi.org/10.1517/17425247.2016.1115835>.
29. Lutton RE, Moore J, Larraneta E, Ligett S, Woolfson AD, Donnelly RF. Microneedle characterisation: the need for universal acceptance criteria and GMP specifications when moving towards commercialisation. *Drug Deliv Transl Res*. 2015;5(4):313–31. <https://doi.org/10.1007/s13346-015-0237-z>.
30. Jeong HR, Lee HS, Choi IJ, Park JH. Considerations in the use of microneedles: pain, convenience, anxiety and safety. *J Drug Target*. 2017;25(1):29–40. <https://doi.org/10.1080/1061186X.2016.1200589>.
31. Bhatnagar S, Dave K, Venuganti VVK. Microneedles in the clinic. *J Control Release*. 2017;260:164–82. <https://doi.org/10.1016/j.jconrel.2017.05.029>.
32. Korkmaz E, Friedrich EE, Ramadan MH, Erdos G, Mathers AR, Burak Ozdoganlar O, et al. Therapeutic intradermal delivery of tumor necrosis factor-alpha antibodies using tip-loaded dissolvable microneedle arrays. *Acta Biomater*. 2015;24:96–105. <https://doi.org/10.1016/j.actbio.2015.05.036>.
33. Allen EA, O'Mahony C, Cronin M, O'Mahony T, Moore AC, Crean AM. Dissolvable microneedle fabrication using piezoelectric dispensing technology. *Int J Pharm*. 2016;500(1–2):1–10. <https://doi.org/10.1016/j.ijpharm.2015.12.052>.
34. Kim JD, Kim M, Yang H, Lee K, Jung H. Droplet-born air blowing: novel dissolving microneedle fabrication. *J Control Release*. 2013;170(3):430–6. <https://doi.org/10.1016/j.jconrel.2013.05.026>.
35. Vecchione R, Coppola S, Esposito E, Casale C, Vespini V, Grilli S, et al. Electro-drawn drug-loaded biodegradable polymer microneedles as a viable route to hypodermic injection. *Adv Funct Mater*. 2014;24(23):3515–23. <https://doi.org/10.1002/adfm.201303679>.
36. Lee K, Jung H. Drawing lithography for microneedles: a review of fundamentals and biomedical applications. *Biomaterials*. 2012;33(30):7309–26. <https://doi.org/10.1016/j.biomaterials.2012.06.065>.
37. Lim SH, Ng JY, Kang L. Three-dimensional printing of a microneedle array on personalized curved surfaces for dual-pronged treatment of trigger finger. *Biofabrication*. 2017;9(1):015010. <https://doi.org/10.1088/1758-5090/9/1/015010>.
38. Johnson AR, Caudill CL, Tumbleston JR, Bloomquist CJ, Moga KA, Ermoshkin A, et al. Single-step fabrication of computationally designed microneedles by continuous liquid interface production. *PLoS One*. 2016;11(9):e0162518. <https://doi.org/10.1371/journal.pone.0162518>.
39. Ross S, Scoutaris N, Lamprou D, Mallinson D, Douroumis D. Inkjet printing of insulin microneedles for transdermal delivery. *Drug Deliv Transl Res*. 2015;5(4):451–61. <https://doi.org/10.1007/s13346-015-0251-1>.
40. Uddin MJ, Scoutaris N, Klepetsanis P, Chowdhry B, Prausnitz MR, Douroumis D. Inkjet printing of transdermal microneedles for the delivery of anticancer agents. *Int J Pharm*. 2015;494(2):593–602. <https://doi.org/10.1016/j.ijpharm.2015.01.038>.
41. Boehm RD, Jaipan P, Skoog SA, Staflieni S, VanderWal L, Narayan RJ. Inkjet deposition of itraconazole onto poly(glycolic acid) microneedle arrays. *Biointerphases*. 2016;11(1):011008. <https://doi.org/10.1116/1.4941448>.
42. Saurer EM, Flessner RM, Sullivan SP, Prausnitz MR, Lynn DM. Layer-by-layer assembly of DNA- and protein-containing films on microneedles for drug delivery to the skin. *Biomacromolecules*. 2010;11(11):3136–43. <https://doi.org/10.1021/bm1009443>.
43. DeMuth PC, Moon JJ, Suh H, Hammond PT, Irvine DJ. Releasable layer-by-layer assembly of stabilized lipid nanocapsules on microneedles for enhanced transcutaneous vaccine delivery. *ACS Nano*. 2012;6(9):8041–51. <https://doi.org/10.1021/nn302639r>.
44. DeMuth PC, Min YJ, Huang B, Kramer JA, Miller AD, Barouch DH, et al. Polymer multilayer tattooing for enhanced DNA vaccination. *Nat Mater*. 2013;12(4):367–76. <https://doi.org/10.1038/NMAT3550>.
45. Prausnitz MR. Microneedles for transdermal drug delivery. *Adv Drug Deliv Rev*. 2004;56(5):581–7. <https://doi.org/10.1016/j.addr.2003.10.023>.
46. Gupta J, Park SS, Bondy B, Felner EI, Prausnitz MR. Infusion pressure and pain during microneedle injection into skin of human subjects. *Biomaterials*. 2011;32(28):6823–31. <https://doi.org/10.1016/j.biomaterials.2011.05.061>.
47. Bodhale DW, Nisar A, Afzulpurkar N. Structural and microfluidic analysis of hollow side-open polymeric microneedles for transdermal drug delivery applications. *Microfluid Nanofluid*. 2010;8(3):373–92. <https://doi.org/10.1007/s10404-009-0467-9>.
48. Sullivan SP, Murthy N, Prausnitz MR. Minimally invasive protein delivery with rapidly dissolving polymer microneedles. *Adv Mater*. 2008;20(5):933–8. <https://doi.org/10.1002/adma.200701205>.
49. Park JH, Allen MG, Prausnitz MR. Polymer microneedles for controlled-release drug delivery. *Pharm Res*. 2006;23(5):1008–19. <https://doi.org/10.1007/s11095-006-0028-9>.
50. Gill HS, Prausnitz MR. Coated microneedles for transdermal delivery. *J Control Release*. 2007;117(2):227–37. <https://doi.org/10.1016/j.jconrel.2006.10.017>.
51. Ma Y, Boese SE, Luo Z, Nitin N, Gill HS. Drug coated microneedles for minimally-invasive treatment of oral carcinomas: development and in vitro evaluation. *Biomed Microdevices*. 2015;17(2):1–14. <https://doi.org/10.1007/s10544-015-9944-y>.
52. Donnelly RF, McCrudden MT, Zaid Alkilani A, Larraneta E, McAlister E, Courtenay AJ, et al. Hydrogel-forming microneedles prepared from “super swelling” polymers combined with lyophilised wafers for transdermal drug delivery. *PLoS One*. 2014;9(10):e111547. <https://doi.org/10.1371/journal.pone.0111547>.
53. Donnelly RF, Singh TRR, Garland MJ, Migalska K, Majithiya R, McCrudden CM, et al. Hydrogel-forming microneedle arrays for enhanced transdermal drug delivery. *Adv Funct Mater*. 2012;22(23):4879–90. <https://doi.org/10.1002/adfm.201200864>.
54. Romanyuk AV, Zvezdin VN, Samant P, Grenader MI, Zemlyanova M, Prausnitz MR. Collection of analytes from

- microneedle patches. *Anal Chem.* 2014;86(21):10520–3. <https://doi.org/10.1021/ac503823p>.
55. McCrudden MT, Alkilani AZ, McCrudden CM, McAlister E, McCarthy HO, Woolfson AD, et al. Design and physicochemical characterisation of novel dissolving polymeric microneedle arrays for transdermal delivery of high dose, low molecular weight drugs. *J Control Release.* 2014;180:71–80. <https://doi.org/10.1016/j.jconrel.2014.02.007>.
 56. Chu LY, Choi SO, Prausnitz MR. Fabrication of dissolving polymer microneedles for controlled drug encapsulation and delivery: bubble and pedestal microneedle designs. *J Pharm Sci.* 2010;99(10):4228–38. <https://doi.org/10.1002/jps.22140>.
 57. Ito Y, Yamazaki T, Sugioka N, Takada K. Self-dissolving micropile array tips for percutaneous administration of insulin. *J Mater Sci Mater Med.* 2010;21(2):835–41. <https://doi.org/10.1007/s10856-009-3923-x>.
 58. Ameri M, Daddona PE, Maa Y-F. Demonstrated solid-state stability of parathyroid hormone PTH(1–34) coated on a novel transdermal microprojection delivery system. *Pharm Res.* 2009;26(11):2454–63. <https://doi.org/10.1007/s11095-009-9960-9>.
 59. Quan FS, Kim YC, Yoo DG, Compans RW, Prausnitz MR, Kang SM. Stabilization of influenza vaccine enhances protection by microneedle delivery in the mouse skin. *PLoS One.* 2009;4(9):e7152. <https://doi.org/10.1371/journal.pone.0007152>.
 60. Donnelly RF, Morrow DIJ, McCrudden MTC, Alkilani AZ, Vicente-Pérez EM, O'Mahony C, et al. Hydrogel-forming and dissolving microneedles for enhanced delivery of photosensitizers and precursors. *Photochem Photobiol.* 2014;90(3):641–7. <https://doi.org/10.1111/php.12209>.
 61. Caffarel-Salvador E, Tuan-Mahmood TM, McElnay JC, McCarthy HO, Mooney K, Woolfson AD, et al. Potential of hydrogel-forming and dissolving microneedles for use in paediatric populations. *Int J Pharm.* 2015;489(1–2):158–69. <https://doi.org/10.1016/j.ijpharm.2015.04.076>.
 62. Doppalapudi S, Jain A, Khan W, Domb AJ. Biodegradable polymers—an overview. *Polym Adv Technol.* 2014;25(5):427–35. <https://doi.org/10.1002/pat.3305>.
 63. Garland MJ, Singh TRR, Woolfson AD, Donnelly RF. Electrically enhanced solute permeation across poly(ethylene glycol)-crosslinked poly(methyl vinyl ether-co-maleic acid) hydrogels: effect of hydrogel crosslink density and ionic conductivity. *Int J Pharm.* 2011;406(1):91–8. <https://doi.org/10.1016/j.ijpharm.2011.01.002>.
 64. Singh TRR, Garland MJ, Migalska K, Salvador EC, Shaikh R, McCarthy HO, et al. Influence of a pore-forming agent on swelling, network parameters, and permeability of poly(ethylene glycol)-crosslinked poly(methyl vinyl ether-co-maleic acid) hydrogels: application in transdermal delivery systems. *J Appl Polym Sci.* 2012;125(4):2680–94. <https://doi.org/10.1002/app.36524>.
 65. Wei M, Gao Y, Li X, Serpe MJ. Stimuli-responsive polymers and their applications. *Polym Chem.* 2017;8(1):127–43. <https://doi.org/10.1039/c6py01585a>.
 66. Rancan F. Biodegradable, biocompatible, and bioconjugate materials as delivery agents in dermatology 2016:73–87. <https://doi.org/10.1016/b978-0-12-802926-8.00006-9>.
 67. Torrisi BM, Zarnitsyn V, Prausnitz MR, Anstey A, Gateley C, Birchall JC, et al. Pocketed microneedles for rapid delivery of a liquid-state botulinum toxin in a formulation into human skin. *J Control Release.* 2013;165(2):146–52. <https://doi.org/10.1016/j.jconrel.2012.11.010>.
 68. Kochhar JS, Quek TC, Soon WJ, Choi J, Zou S, Kang L. Effect of microneedle geometry and supporting substrate on microneedle array penetration into skin. *J Pharm Sci.* 2013;102(11):4100–8. <https://doi.org/10.1002/jps.23724>.
 69. Demir YK, Akan Z, Kerimoglu O. Characterization of polymeric microneedle arrays for transdermal drug delivery. *PLoS One.* 2013;8(10):e77289. <https://doi.org/10.1371/journal.pone.0077289>.
 70. Olatunji O, Das DB, Garland MJ, Belaid L, Donnelly RF. Influence of array interspacing on the force required for successful microneedle skin penetration: theoretical and practical approaches. *J Pharm Sci.* 2013;102(4):1209–21. <https://doi.org/10.1002/jps.23439>.
 71. Chu LY, Prausnitz MR. Separable arrowhead microneedles. *J Control Release.* 2011;149(3):242–9. <https://doi.org/10.1016/j.jconrel.2010.10.033>.
 72. Tu J, Du G, Reza Nejadnik M, Monkare J, van der Maaden K, Bomans PHH, et al. Mesoporous silica nanoparticle-coated microneedle arrays for intradermal antigen delivery. *Pharm Res.* 2017;34(8):1693–706. <https://doi.org/10.1007/s11095-017-2177-4>.
 73. Vassilieva EV, Kalluri H, McAllister D, Taherbhai MT, Esser ES, Pewin WP, et al. Improved immunogenicity of individual influenza vaccine components delivered with a novel dissolving microneedle patch stable at room temperature. *Drug Deliv Transl Res.* 2015;5(4):360–71. <https://doi.org/10.1007/s13346-015-0228-0>.
 74. Park JH, Choi SO, Kamath R, Yoon YK, Allen MG, Prausnitz MR. Polymer particle-based micromolding to fabricate novel microstructures. *Biomed Microdevices.* 2007;9(2):223–34. <https://doi.org/10.1007/s10544-006-9024-4>.
 75. McAllister DV, Allen MG, Prausnitz MR. Microfabricated microneedles for gene and drug delivery. *Annu Rev Biomed Eng.* 2000;2(1):289–313. <https://doi.org/10.1146/annurev.bioeng.2.1.289>.
 76. McAllister DV, Wang PM, Davis SP, Park J-H, Canatella PJ, Allen MG, et al. Microfabricated needles for transdermal delivery of macromolecules and nanoparticles: fabrication methods and transport studies. *Proc Natl Acad Sci U S A.* 2003;100(24):13755–60. <https://doi.org/10.1073/pnas.2331316100>.
 77. Yang S, Wu F, Liu J, Fan G, Welsh W, Zhu H, et al. Phase-transition microneedle patches for efficient and accurate transdermal delivery of insulin. *Adv Funct Mater.* 2015;25(29):4633–41. <https://doi.org/10.1002/adfm.201500554>.
 78. Kim M, Jung B, Park JH. Hydrogel swelling as a trigger to release biodegradable polymer microneedles in skin. *Biomaterials.* 2012;33(2):668–78. <https://doi.org/10.1016/j.biomaterials.2011.09.074>.
 79. Wang QL, Zhu DD, Liu XB, Chen BZ, Guo XD. Microneedles with controlled bubble sizes and drug distributions for efficient transdermal drug delivery. *Sci Rep.* 2016;6(1):38755. <https://doi.org/10.1038/srep38755>.
 80. van der Maaden K, Lutge R, Vos PJ, Bouwstra J, Kersten G, Ploemen I. Microneedle-based drug and vaccine delivery via nanoporous microneedle arrays. *Drug Deliv Transl Res.* 2015;5(4):397–406. <https://doi.org/10.1007/s13346-015-0238-y>.
 81. Mascia S, Heider PL, Zhang H, Lakerveld R, Benyahia B, Barton PI, et al. End-to-end continuous manufacturing of pharmaceuticals: integrated synthesis, purification, and final dosage formation. *Angew Chem Int Ed.* 2013;52(47):12359–63. <https://doi.org/10.1002/anie.201305429>.
 82. Daly R, Harrington TS, Martin GD, Hutchings IM. Inkjet printing for pharmaceuticals—a review of research and manufacturing. *Int J Pharm.* 2015;494(2):554–67. <https://doi.org/10.1016/j.ijpharm.2015.03.017>.
 83. Schleis TG. Interference of maltose, icodextrin, galactose, or xylose with some blood glucose monitoring systems. *Pharmacother: The J Human Pharmacol Drug Ther.* 2007;27(9):1313–21. <https://doi.org/10.1592/phco.27.9.1313>.

84. Goole J, Amighi K. 3D printing in pharmaceuticals: a new tool for designing customized drug delivery systems. *Int J Pharm.* 2016;499(1):376–94. <https://doi.org/10.1016/j.ijpharm.2015.12.071>.
85. Urwyler P, Pascual A, Müller B, Schiff H. Ultraviolet–ozone surface cleaning of injection-molded, thermoplastic microcantilevers. *Journal of Applied Polymer Science.* 2015;132(18):n/a-n/a. doi: <https://doi.org/10.1002/app.41922>.
86. Nerandzic MM, Cadnum JL, Pultz MJ, Donskey CJ. Evaluation of an automated ultraviolet radiation device for decontamination of *Clostridium difficile* and other healthcare-associated pathogens in hospital rooms. *BMC Infect Dis.* 2010;10(1):197. <https://doi.org/10.1186/1471-2334-10-197>.
87. Montenegro-Nicolini M, Miranda V, Morales JO. Inkjet printing of proteins: an experimental approach. *AAPS J.* 2017;19(1):234–43. <https://doi.org/10.1208/s12248-016-9997-8>.
88. Boehm RD, Miller PR, Hayes SL, Monteiro-Riviere NA, Narayan RJ. Modification of microneedles using inkjet printing. *AIP Adv.* 2011;1(2):22139. <https://doi.org/10.1063/1.3602461>.
89. McCrudden MT, Alkilani AZ, Courtenay AJ, McCrudden CM, McCloskey B, Walker C, et al. Considerations in the sterile manufacture of polymeric microneedle arrays. *Drug Deliv Transl Res.* 2015;5(1):3–14. <https://doi.org/10.1007/s13346-014-0211-1>.
90. DeMuth PC, Su X, Samuel RE, Hammond PT, Irvine DJ. Nanolayered microneedles for transcutaneous delivery of polymer nanoparticles and plasmid DNA. *Adv Mater.* 2010;22(43):4851–6. <https://doi.org/10.1002/adma.201001525>.
91. Melocchi A, Parietti F, Maroni A, Foppoli A, Gazzaniga A, Zema L. Hot-melt extruded filaments based on pharmaceutical grade polymers for 3D printing by fused deposition modeling. *Int J Pharm.* 2016;509(1):255–63. <https://doi.org/10.1016/j.ijpharm.2016.05.036>.
92. Wang F, Shor L, Darling A, Khalil S, Sun W, Guceri S, et al. Precision extruding deposition and characterization of cellular poly-epsilon-caprolactone tissue scaffolds. *Rapid Prototyp J.* 2004;10(1):42–9. <https://doi.org/10.1108/13552540410512525>.
93. Kim JH, Je K, Shim TS, Kim SH. Reaction–diffusion-mediated photolithography for designing pseudo-3D microstructures. *Small.* 2017;13(17). doi:<https://doi.org/10.1002/sml.201603516>.
94. Gupta J, Gill HS, Andrews SN, Prausnitz MR. Kinetics of skin resealing after insertion of microneedles in human subjects. *J Control Release.* 2011;154(2):148–55. <https://doi.org/10.1016/j.jconrel.2011.05.021>.
95. Gupta J, Denson DD, Felner EI, Prausnitz MR. Rapid local anesthesia in human subjects using minimally invasive microneedles. *Clin J Pain.* 2012;28(2):129–35. <https://doi.org/10.1097/AJP.0b013e318225dbe9>.
96. Hirobe S, Azukizawa H, Hanafusa T, Matsuo K, Quan YS, Kamiyama F, et al. Clinical study and stability assessment of a novel transcutaneous influenza vaccination using a dissolving microneedle patch. *Biomaterials.* 2015;57:50–8. <https://doi.org/10.1016/j.biomaterials.2015.04.007>.
97. Kaushik S, Hord AH, Denson DD, McAllister DV, Smitra S, Allen MG, et al. Lack of pain associated with microfabricated microneedles. *Anesth Analg.* 2001;92(2):502–4. <https://doi.org/10.1213/0000539-200102000-00041>.
98. Kelchen MN, Siefers KJ, Converse CC, Farley M, Holdren GO, Brogdena NK. Micropore closure kinetics are delayed following microneedle insertion in elderly subjects. *J Control Release.* 2016;225:294–300. <https://doi.org/10.1016/j.jconrel.2016.01.051>.
99. Baek C, Han M, Min J, Prausnitz MR, Park JH, Park JH. Local transdermal delivery of phenylephrine to the anal sphincter muscle using microneedles. *J Control Release.* 2011;154(2):138–47. <https://doi.org/10.1016/j.jconrel.2011.05.004>.
100. Donnelly RF, Singh TRR, Alkilani AZ, McCrudden MTC, O’Neill S, O’Mahony C, et al. Hydrogel-forming microneedle arrays exhibit antimicrobial properties: potential for enhanced patient safety. *Int J Pharm.* 2013;451(1):76–91. <https://doi.org/10.1016/j.ijpharm.2013.04.045>.
101. Vicente-Perez EM, Larraneta E, McCrudden MTC, Kissenpennig A, Hegarty S, McCarthy HO et al. Repeat application of microneedles does not alter skin appearance or barrier function and causes no measurable disturbance of serum biomarkers of infection, inflammation or immunity in mice in vivo. *Eur J Pharm Biopharm* 2017;117:400–407. doi:<https://doi.org/10.1016/j.ejpb.2017.04.029>.
102. Center for Biologics Evaluation and Research. Guidance for industry: nonclinical studies for the safety evaluation of pharmaceutical excipients. Rockville, MD: Food and Drug Administration; 2005 [cited on 2017 Dec 1]. 12 p. Available from: <https://www.fda.gov/ohrms/dockets/98fr/2002d-0389-gdl0002.pdf>
103. Donnelly RF, Garland MJ, Morrow DI, Migalska K, Singh TR, Majithiya R, et al. Optical coherence tomography is a valuable tool in the study of the effects of microneedle geometry on skin penetration characteristics and in-skin dissolution. *J Control Release.* 2010;147(3):333–41. <https://doi.org/10.1016/j.jconrel.2010.08.008>.
104. Kochhar JS, Goh WJ, Chan SY, Kang L. A simple method of microneedle array fabrication for transdermal drug delivery. *Drug Dev Ind Pharm.* 2013;39(2):299–309. <https://doi.org/10.3109/03639045.2012.679361>.